Inorg. Chem. **2004**, *43*, 3225–3229

An Evaluation by Density Functional Theory of M–M Interactions in Organometallic Clusters with the $[Fe_3MoS_3]^{2+}$ Cores

Paola Nava,[†] Jaehong Han,[‡] Reinhart Ahlrichs,*[,†] and Dimitri Coucouvanis*[,‡]

Departments of Chemistry, University of Karlsruhe, Karlsruhe, Germany, and University of Michigan, Ann Arbor, Michigan 48109-1055

Received January 14, 2004

Density functional theory calculations were carried out on the structurally characterized $[(Cl_4\text{-cat})Mo(py)Fe_3S_3(CO)_4(P^nPr_3)_3]$, **A**, and $(Cl_4\text{-cat})Mo(py)Fe_3S_3(CO)_6(PEt_3)_2$, **B**, and also on $\mathbf{A}^{2-}$ and $\mathbf{B}^{2+}$clusters. The Fe–Fe distances in these molecules depend on the total number of valence electrons (60 e^- in **A** and $\mathbf{B}^{2+}$ and 62 e^- in $\mathbf{A}^{2-}$ and **B**) and undergo great structural changes upon addition or removal of electrons. The changes are consistent with known electron-counting rules in organometallic chemistry. The weak nature of the Fe–Fe bonding interactions in these clusters is apparent in the very similar energies of states with widely different Fe–Fe distances.

In our search of synthetic structural analogues for the nitrogenase Fe/Mo/S site we have obtained a series of clusters that contain the $MoFe_3S_3$ core as a common structural unit.[1] These units structurally resemble the Mo bearing cuboidal subunit within the $MoFe_7S_9$ core in the cofactor of nitrogenase.[2−5] The structures of the $[(Cl_4\text{-cat})Mo(py)Fe_3S_3(CO)_4(P^nPr_3)_3]$, **A**, and $(Cl_4\text{-cat})Mo(py)Fe_3S_3(CO)_6(PEt_3)_2$, **B**, clusters ($Cl_4$-cat = tetrachlorocatechol) have been determined[1] (Figure 1). The isolation of **A** and **B** in only small quantities has precluded the synthesis of reduced or oxidized derivatives of these compounds. Clusters **A** and **B** both contain a pyridine and a catecholate, bidentate chelating ligand bound to the Mo atom and three triply bridging sulfido ligands integral to the cuboidal $MoFe_3S_3$ subunit. Cluster **A** contains seven two-electron donor terminal ligands distributed into two $(\mu_3\text{-}S)_2(L)_2Fe$ and one $(\mu_3\text{-}S)_2(L)_3Fe$ units. Cluster **B** with eight terminal ligands contains two $(\mu_3\text{-}S)_2(L)_3Fe$ and one $(\mu_3\text{-}S)_2(L)_2Fe$ units. The total number of ligand electrons that participate in M−ligand bonding are 38 for **A** and 40 for **B**. The neutral clusters must contain $[Fe_3Mo]^{+8}$ central units to balance the ligand charges of −8 (three S^{2-} and cat^{2-}). Possible combinations of oxidation states for an 8^+ charge are $Mo^{2+}(Fe^{2+})_3$, $Mo^{3+}(Fe^{2+})_2(Fe^{1+})$, or even Mo^{4+} $(Fe^{1+})_2(Fe^{2+})$. In the absence of magnetic studies and detailed Moessbauer data for the closed-shell **A** and **B**, it is not possible to make a definitive choice among the above combinations. For any of these possibilities, however, the total number of metal d electrons is 22, and therefore, the total numbers of valence electrons for **A** and **B**, respectively, are 60 and 62. Various electron counting schemes[6] predict that, in the $MoFe_3S_3$ clusters, a total of 60 valence electrons will lead to a completely M−M bonded M_4 tetrahedron. The mean Fe−Fe and Fe−Mo distances in the 60 valence electron **A** are 2.59 and 2.73 Å, respectively, and can be considered as M−M single bonds. As additional valence electrons are added to the $MoFe_3S_3$ clusters, the M−M bonding is expected to weaken. In **B**, the total number of valence electrons is 62. In this molecule (Figure 1B) the structure shows mean Fe−Fe and Fe−Mo distances of 3.00 and 2.77 Å, respectively. The increased average Fe−Fe distance is due to the lengthening of one of the Fe−Fe distances (Fe_1−Fe_3) to a nonbonding separation of 3.62 Å.

In **B** (Figure 1B), the elongated Fe−Fe distance between the five-coordinate Fe atoms could be partly attributed to a combination of both the higher 62 electron count and coordination "crowding". The relative contributions of these two effects remain to be established. In the absence of

* To whom correspondence should be addressed. E-mail: dcouc@umich.edu (D.C.).
[†] University of Karlsruhe.
[‡] University of Michigan.

(1) (a) Coucouvanis, D.; Han, J.; Moon, N. *J. Am. Chem. Soc.* **2002**, *124*, 216. (b) Han, J.; Beck, K.; Ockwig, N.; Coucouvanis, D. *J. Am. Chem. Soc.* **1999**, *121*, 10448.
(2) (a) Kim, J.; Rees, D. C. *Nature* **1992**, *360*, 553. (b) Peters J. W.; Stowell, M. H. B.; Soltis, S. M.; Finnegan, M. G.; Johnson, M. K.; Rees, D. C. *Biochemistry* **1997**, *36*, 1181 and references therein.
(3) Bolin, J. T.; Ronco, A. E.; Morgan, T. V.; Mortenson, L. E.; Xuong, N. *Proc. Natl. Acad. Sci. U. S.A.* **1993**, *90*, 1078.
(4) Mayer, S. M.; Lawson, D. M.; Gormal, C. A.; Roe, S. M.; Smith, B. E. *J. Mol. Biol.* **1999**, *292*, 871.
(5) Einsle, O.; Tezcan, A. F.; Andrade, S. L. A.; Schmid, B.; Yoshida, M.; Howard, J. B.; Rees, D. C. *Science* **2002**, *297*, 1696−1700.
(6) Michael, D.; Mingos, P.; May, A. S. Structure and Bonding Aspects of Metal Cluster Chemistry. In *Chemistry of Metal Cluster Complexes*; Shriver, D. F.; Kaesz, H. D.; Adams, R. D., Eds.; VCH: New York, 1990; Chapter 2, pp 81−114.

10.1021/ic0499392 CCC: $27.50
Published on Web 04/14/2004

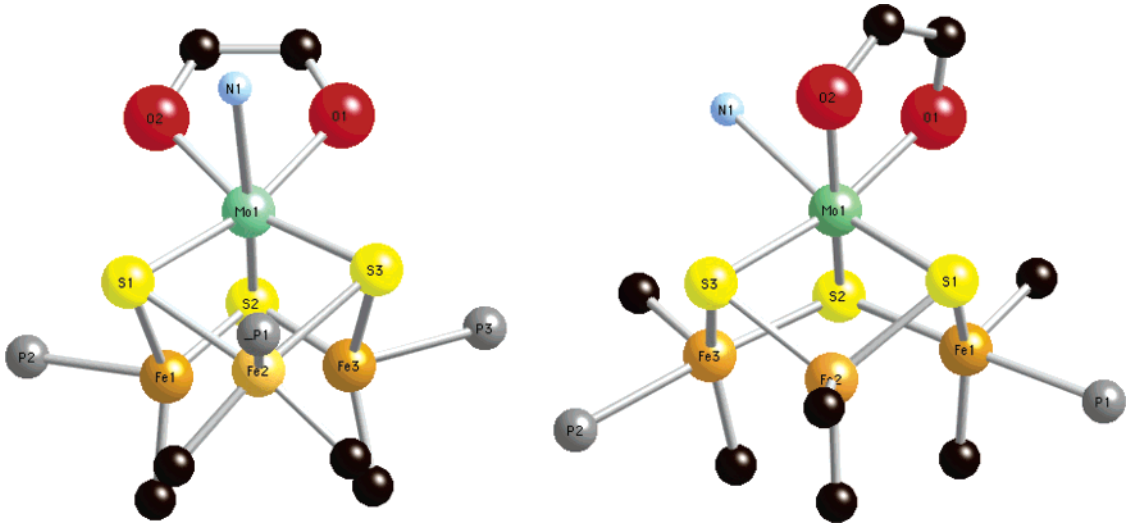

Figure 1. Crystal structures of the $[(Cl_4\text{-cat})Mo(py)Fe_3S_3(CO)_4(P^nPr_3)_3]$, **A**, and $(Cl_4\text{-cat})Mo(py)Fe_3S_3(CO)_6(PEt_3)_2$, **B**, clusters. For clarity only the carbon atoms attached to the tetrachlorocatecholate ligands are shown. Also hidden are the alkyl groups on the PR_3 ligands, the oxygen atoms of the carbonyl ligands, and the carbon atoms of the Mo-coordinated pyridine ligands.

structure determinations for either the two-electron oxidized **B** or the two-electron reduced **A** clusters, it is not possible to evaluate the decrease in M−M bonding in the former or the corresponding increase of M−M bonding in the latter, strictly on valence electron counting considerations.

An evaluation of M−M interactions and the optimization of the oxidized and reduced cluster structures, maintaining the same number of terminally coordinated ligands, is possible by density functional theory (DFT) calculations. A DFT study of **A** and **B** was therefore undertaken.

The presence, and relative strength, of M−M bonds in multimetallic clusters often is an issue that must be resolved on the basis of accurate theoretical calculations or appropriate experimental data. A detailed general understanding of M−M interactions is particularly desirable for certain biologically important multimetallic clusters, such as the FeMo cofactor in nitrogenase, where unusually short M−M distances are found[2−5] and may play a role in catalysis.

Various quantum mechanical calculations have appeared in the literature and are concerned with the detailed electronic structural description of the FeMo-cofactor of nitrogenase[7] or with the nature of the cofactor−substrate interactions.[7b−f] In some of these studies[7a−c] some discussions concerning M−M interactions and their strength have been presented.

The calculations reported herein were performed with the DFT implementation of TURBOMOLE.[9−11] using the BP86 functional.[12−14] Coulomb interactions are treated with the resolution of identity RI-J approximation.[15,16] An SV(P) basis[16,17] (split valence plus polarization, except for H) and an (effective core potential) ECP[18] for the molybdenum atom are used. Test calculations with TZVP basis[16] (triple-ζ valence plus polarization) led to virtually the same results.

A general problem that one encounters in theoretical treatments of clusters such as **A** or **B** is that the spin states and, in the case of molecular symmetry (beyond C_1), the occupation patterns are not known a priori. To locate the electronic ground state within a given method of calculations, i.e., a given functional, one has to vary spin distribution and MO occupation of each molecular structure. For this purpose Fermi smearing[19] has been employed,[20] which is based on the use of noninteger occupations for MOs of α and β spin. Molecular orbitals and occupation numbers are then varied simultaneously during the SCF iteration procedure. In the present case this always resulted in integer occupation for spin-orbitals. Although there is no guarantee that the correct electronic state has actually been found, we are confident to have succeeded in this respect since calculations using different MOs and molecular structures as a start converge to the same result.

Calculations were carried out for two representative clusters in the $MoFe_3S_3$ class. In the optimized structure of the reduced $[(Cl_4\text{-cat})Mo(py)Fe_3S_3(L)_7]^{2-}$ cluster $\mathbf{A}^{2-}$ (Table

(7) (a) Lovell, T.; Li, J.; Liu, T.; Case, D. A.; Noodleman, L. *J. Am. Chem. Soc.* **2001**, *123*, 12392−12410. (b) Deng, H.; Hoffman, R. *Angew. Chem., Int. Ed. Engl.* **1993**, *32*, 1062. (c) Dance, I. *Aust. J. Chem.* **1994**, *47*, 979. (d) Stavrev, K. K.; Zerner, M. C. *Chem. Eur. J.* **1996**, *2*, 83 (e) Stavrev, K. K.; Zerner, M. C. *Theor. Chim. Acta* **1997**, *96*, 141. (f) Stavrev, K. K.; Zerner, M. C. *Int. J. Quantum Chem.* **1998**, *1*, 581. (g) Durrant, M. C. *Biochemistry* **2002**, *41*, 13934. (h) Durrant, M. C. *Biochemistry* **2002**, *41*, 13946.
(8) (a) Hinnemann, B.; Norskov, J. K. *J. Am. Chem. Soc.* **2003**, *125*, 1466. (b) Dance, I. *J. Chem. Soc., Chem. Commun.* **2003**, 324.
(9) Ahlrichs, R.; Baer, M.; Horn, H.; Koelmel, Ch. *Chem. Phys. Lett.* **1989**, *162*, 165.
(10) Haeser, M.; Ahlrichs, R. *J. Comput. Chem.* **1989**, *10*, 104.
(11) von Arnim, M.; Ahlrichs, R. *J. Comput. Chem.* **1998**, *19*, 1746.
(12) Perdew, J. P. *Phys. Rev. B* **1986**, *33*, 8822−8824.
(13) Perdew, J. P. *Phys. Rev. B* **1986**, *34*, 7046.
(14) Becke, A. D. *Phys. Rev. A* **1988**, *34*, 7046.
(15) Eichkorn, K.; Treutler, O.; Oehm, H.; Haeser, M.; Ahlrichs, R. *Chem. Phys. Lett.* **1995**, *240*, 283.
(16) Eichkorn, K.; Weigend, F.; Treutler, O.; Ahlrichs, R. *Theor. Chem. Acc.* **1997**, *97*, 119.
(17) Schaefer, A.; Horn, H.; Ahlrichs, R. *J. Chem. Phys.* **1992**, *97*, 2571.
(18) Andrae, D.; Haeussermann, U.; Dolg, M.; Stoll, H.; Preuss, H. *Theor. Chim. Acta* **1990**, *77*, 123.
(19) Dunlap, B. I.; Mei, W. N. *J. Chem. Phys.* **1983**, *78*, 4997.
(20) The present procedure is technically slightly different since we use the error function instead of the exponential $n_i = {}^1/_2 erfc(\epsilon_i - \mu)/fT$, in the usual nomenclature. The "temperature" T is set to 300 K at the start and is gradually reduced to 100 K during SCF iterations, which is based on the use of noninteger occupations for MOs of α and β spin.

Table 1. Computed Bond Lengths (Å) of the Neutral (60 e^-) and the Reduced (62 e^-) Forms of **A**[a]

	neutral molecule				reduced molecule	
bond	expt	$^3A''$	$^1A'$[b]	$^1A'$[c]	$^1A'$	$^3A''$
Fe_1-Fe_3	2.590(5)	2.717	2.550	3.379	3.205	2.606
Fe_1-Fe_2	2.600(8) 2.590(2)[d]	2.517	2.481	2.456	2.485	2.574
Fe_1-S_1	2.196(9) 2.208(2)	2.288	2.266	2.293	2.332	2.287
Fe_1-S_2	2.190(2)	2.200	2.194	2.208	2.240	2.224
Fe_2-S_1	2.292(9)	2.356	2.325	2.351	2.352	2.384
Fe_2-S_2	3.842	3.721	3.785	3.150	3.399	3.935
$Mo-Fe_1$	2.651(1)	2.692	2.665	2.809	2.739	2.421
$Mo-Fe_2$	2.883(4)	2.872	2.928	2.667	2.776	3.292
Fe_1-C_1	1.783(7)	1.785	1.794	1.851	1.845	1.766
Fe_3-C	1.792(4)	2.441	2.498	2.018	2.058	2.553
Fe_1-P	2.253(5)	2.134	2.201	2.201	2.134	2.159
Fe_2-P	2.26(2)	2.196	2.213	2.197	2.133	2.135

[a] In the DFT calculations, both PH_3 and PMe_3 were used as PR_3 ligands. No significant differences were found, and PH_3 was used in subsequent calculations. It was assumed that Fe_2 lies on a mirror plane of symmetry that relates Fe_1 and Fe_3 (the calculations were based on a model with C_s point group symmetry). Experimental data for neutral **A** ($(Cl_4$-cat)Mo(py)$Fe_3S_3(CO)_4(P^nPr_3)_3$) also are included. The numbering scheme follows Figure 1. [b] The HOMO has a′ symmetry. [c] The HOMO has a″ symmetry. [d] In the crystal structure, the chemically equivalent Fe_1 and F_3 are not related by symmetry.

Table 2. Computed Bond Lengths (Å) of the Neutral (62 e^-) and the Oxidized (60 e^-) Forms of **B**[a]

	neutral molecule			oxidized molecule	
bond	expt	$^1A'$	$^3A''$	$^3A''$	$^1A'$
Fe_1-Fe_3	3.618	3.566	3.962	2.815	3.564
Fe_1-Fe_2	2.703(1) 2.678(1)[b]	2.608	2.571	2.723	2.616
Fe_1-S_1	2.207(1) 2.221(1)	2.279	2.307	2.295	2.262
Fe_1-S_2	2.295(1)	2.377	2.383	2.300	2.298
Fe_2-S_1	2.194(1)	2.225	2.260	2.226	2.208
Fe_2-S_2	3.332	3.338	3.557	3.826	3.293
$Mo-Fe_1$	2.786(1)	2.932	3.548	2.792	2.840
$Mo-Fe_2$	2.669(1)	2.677	2.710	2.695	3.648

[a] Experimental data for neutral **B**, $(Cl_4$-cat)Mo(py)$Fe_3S_3(CO)_6(PEt_3)_2$, also are reported. The numbering scheme follows Figure 1. [b] In the crystal structure the chemically equivalent Fe_1 and F_3 are not related by symmetry. In the DFT calculations C_s symmetry was assumed.

1), one of the Fe−Fe distances is found at 3.21Å while the other two are Fe−Fe single bonds at 2.49 Å. The crystallographically determined Fe_1-Fe_3 distance in **B** is also nonbonding (3.62 Å). It is 0.42 Å longer than the corresponding distance in $\mathbf{A}^{2-}$, a difference which may reflect in part the greater coordination number (and "crowding") of the two Fe atoms in the Fe_1-Fe_3 pair of **B**. The DFT optimized structure of the oxidized $[(Cl_4$-cat)Mo(py)$Fe_3S_3(L)_8]^{2+}$ cluster $\mathbf{B}^{2+}$ (Table 2) also shows the expected shortening of the long Fe−Fe distance (from 3.62 to 2.82 Å). This distance again is longer than the 2.59 Å distance observed in cluster **A** and is very likely due to the difference in coordination numbers between the corresponding Fe pairs.

In general, the DFT-calculation-optimized structures (with BP86) show slightly longer M−S distances and either longer or shorter M−M distances than the crystallographically determined ones. These differences, often no greater than 0.05 Å, are hardly significant. The data in Table 1 show (Figure 2) a triplet ground state calculated for the neutral **A**

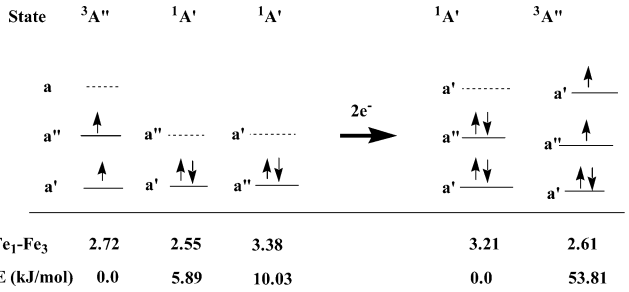

Figure 2. Schematic representations of the HOMO and LUMO shells of the neutral and reduced forms of **A** in singlet and triplet states. Molecular orbitals of a″ symmetry are Fe−Fe antibonding. Molecular orbitals of a′ symmetry are Fe−Fe bonding. The Fe−Fe distances of the Fe_1-Fe_3 pair in different states reflect the nature of the a′ and a″ orbitals. Pictorial representations of HOMO and LUMO orbitals have been deposited.

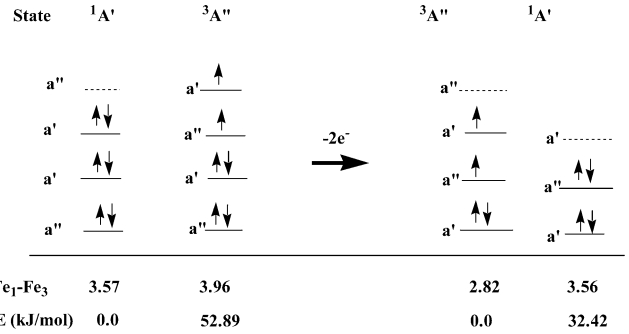

Figure 3. Schematic representations of the HOMO and LUMO shells of the neutral and oxidized forms of **B**. Molecular orbitals of a″ symmetry are Fe−Fe antibonding. Molecular orbitals of a′ symmetry are Fe−Fe bonding (see also Figure 2 caption). Pictorial representations of HOMO and LUMO orbitals have been deposited as Supporting Information.

molecule with singly occupied, bonding (a′), and antibonding (a″) molecular orbitals and an optimized Fe_1-Fe_3 distance of 2.72 Å. A singlet state, with a bonding HOMO of a′ symmetry, is only 5.9 kJ higher in energy with an optimized Fe_1-Fe_3 distance of 2.55 Å. An additional singlet state, with an antibonding HOMO of a″ symmetry at 10.0 kJ higher than the triplet ground state, is associated with an optimized Fe_1-Fe_3 distance of 3.38 Å. Considering that the calculations are performed for the isolated molecules "in vacuo", any of the states shown in Figure 2, for the neutral 60 e^- cluster **A**, could be "reached" readily by ordinary low energy environmental perturbations. Similarly, for the oxidized 60 e^- cluster $\mathbf{B}^{2+}$, the triplet ground state with an Fe_1-Fe_3 distance of 2.82 Å is within 32.4 kJ mol^{-1} from a singlet state with an Fe_1-Fe_3 distance of 2.61 Å (Table 2, Figure 3). These large differences in Fe_1-Fe_3 distances, for states quite similar in energy, lead to the following conclusion: Fe−Fe interactions in **A** and **B** are rather weak[21] and may allow for unusual structural flexibility in these clusters.

The DFT optimized structure for the reduced $[(Cl_4$-cat)-Mo(py)$Fe_3S_3(CO)_4(P^nPr_3)_3]^{2-}$, $\mathbf{A}^{2-}$, cluster and the subsequent elongation of one of the Fe−Fe distances (Table 1, Figure 2) shows an interesting change in the coordination modes of the two terminal CO ligands bound to the central Fe atom. Each of these COs approaches the four-coordinate Fe_1 and Fe_3 atoms and assumes a nearly bridging coordination (Figure 4). This structural change, that remains to be established crystallographically, is the result of the Fe_1-Fe_3

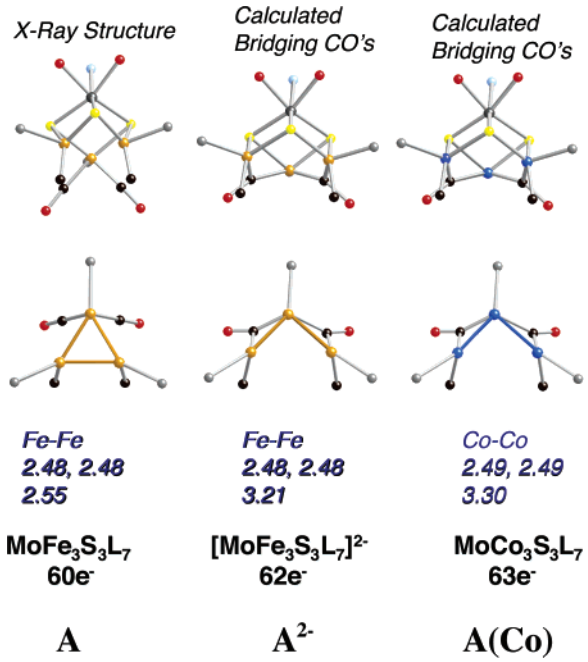

Figure 4. Two views of the crystallographically determined structure of [(Cl_4-cat)Mo(py)$Fe_3S_3(CO)_4(P^nPr_3)_3$], **A**, and the hypothetical $\mathbf{A}^{2-}$ and [(Cl_4-cat)Mo(py)$Co_3S_3(CO)_4(P^nPr_3)_3$] clusters. The trimetallic, triangular bases of these clusters show the structural changes occurring upon reduction.

distance elongation that renders the Fe atoms' coordination unsaturation. The same type of bridging COs is found in the optimized structure of the hypothetical (Cl_4-cat)Mo(py)-$Co_3S_3(L)_7$ cluster (Figure 4), which contains Co atoms in place of Fe and consequently additional valence electrons. The Fe−Fe attractive (bonding) interactions that emerge from crystallographic structure determinations and DFT calculations are further supported in calculations where the S bridging ligands in the $MoFe_3S_3$ clusters are replaced by Se or Te atoms. The optimized structures for the $MoFe_3E_3$ clusters (E = Se, Te) show nearly identical Fe−Fe distances (Table 3) with mean values around 2.50 Å. This is quite significant considering the differences in the Fe−S, Fe−Se, and Fe−Te bonds which have average values of 2.27, 2.40, and 2.63 Å, respectively. As expected, the Fe−Se−Fe and Fe−Te−Fe angles at 68° and 63° are quite acute and apparently strained. In the $[Sn_2Te_6]^{4-}$ dimer,[21] which contains edge-sharing tetrahedral $SnTe_4$ units, and Sn−Sn bonding is not expected, the Sn−Te−Sn angles are 85°. The invariance of the Fe−Fe distances on the replacement S → Se, Te can be rationalized as a result of bonding Fe−Fe interactions, particularly for Fe−Fe distances close to those in Fe metal. Resistance to extension of the M_6 polyhedra in $[M_6E_8(CO)_6]$ clusters (M = Cr, E = S, Se, Te) previously has been considered[22] indicative of (relatively weak) intermetallic bonding. In these clusters, the Cr−Cr distances were calculated at 2.47, 2.52, and 2.60 Å for E = S, Se, and Te, respectively. Interestingly, and as expected, the corresponding Co clusters (with 18 additional valence electrons) did not show invariance in the Co−Co distances. The latter, for the three different E atoms, vary from 2.79(S) to 3.06 (Te) Å and show no M−M bonding interactions. The results presented herein and the increase in M−M bonding interactions, with a decrease in the overall number of valence electrons in organometallic clusters, are in concert with the pioneering structural studies of Dahl and co-workers nearly four decades ago.[23]

Table 3. Structure Optimizations of **A** with S, Se, and Te as μ_3-Ligands[a]

	Singlet State			
	X = S (DFT)	X = Se (DFT)	X = Te (DFT)	X = S (X-ray)
Fe(1)−X(1)	2.27	2.40	2.63	2.196(1), 2.208(2)
Fe(1)−X(2)	2.19	2.32	2.53	2.190(2)
Fe(2)−X(1)	2.33	2.43	2.61	2.292(9)
Fe(2)−X(2)	3.79	3.90	4.07	3.842(9)
Fe(1)−Fe(2)	2.48	2.47	2.43	2.600(8)
Fe(1)−Fe(3)	2.55	2.58	2.62	2.590(5)
Fe(1)−X2−Fe(3)	71.1°	67.8°	62.5°	
	Triplet State			
	X = S (DFT)	X = Se (DFT)	X = Te (DFT)	
Fe(1)−X(1)	2.28	2.42	2.63	
Fe(1)−X(2)	2.20	2.32	2.51	
Fe(2)−X(1)	2.36	2.46	2.65	
Fe(2)−X(2)	3.72	3.80	4.00	
Fe(1)−Fe(2)	2.52	2.49	2.48	
Fe(1)−Fe(3)	2.72	2.77	2.81	
Fe(1)−X2−Fe(3)	76.3°	73.2°	67.9°	

[a] Distances (Å) and Fe(1)−X2−Fe(3) angle for the singlet state, HOMO = a′, and the triplet state, HOMO = a″.

In conclusion, the $[MoFe_3S_3]$ cores in clusters **A** and **B** with 60 e^- and 62 e^-, respectively, show Fe−Fe bonding interactions. These interactions are weak, but persistent. Differences in coordination numbers and geometries for the Fe atoms in **A** and **B** allow for the localization of bonding or antibonding effects within a pair of Fe atoms as the 3Fe triangular units in these clusters interconvert between equilateral and isosceles geometries. The close energy separations between states, with widely different Fe−Fe distances (Figures 2 and 3), show that steric changes, if needed for specific reactivity, may occur readily with a minimum expenditure in energy.

The results presented herein may be of some relevance to the nitrogenase problem. Weak Fe−Fe bonding interactions of the type described above also are present in the $MoFe_6S_9$ core of the nitrogenase cofactor[24,26] and could play a role in the activation and reduction of dinitrogen.

Acknowledgment. D.C. and J.H. acknowledge the continuing support of this research by the NIH (GM33080). In the University of Karlsruhe, this work is supported by the

(21) Dehnen, S.; Zimmermann, C.; Anson, C. E. *Z. Anorg. Allg. Chem.* **2002**, *628*, 279.
(22) Fan, P.-D.; Deglmann, P.; Ahlrichs, R. *Chem. Eur. J.* **2002**, *8*, 1059−1067.
(23) (a) Dahl, L. F.; Wei, C. H. *Inorg. Chem.* **1963**, *2*, 328. (b) Wei, C. H.; Dahl, L. F. *Inorg. Chem.* **1965**, *4*, 1. (c) Dahl, L. F.; Sutton, P. W. *Inorg. Chem.* **1963**, *2*, 1067.
(24) DFT calculations on the nitrogenase cofactor, including the recently observed central light atom, are reported elsewhere.[25]
(25) Huniar, U.; Ahlrichs, R.; Coucouvanis, D. *J. Am. Chem. Soc.* **2004**, *126*, 2588−2601.
(26) A weak type of Fe−Fe interactions in the cofactor of nitrogenase, has been reported in a recent DFT study. See ref 8 above.

Center for Functional Nanostructures (CFN) of the Deutsche Forschungsgemeinschaft (DFG) within project C2.2. D.C. is indebted to the chemistry faculty in the University of Karlsruhe for their exquisite hospitality during his latest sabbatical leave there.

Supporting Information Available: Tables 3 and 4 with structure optimization of **A** with S, Se, and Te as μ_3-ligands. Distances and Fe(1)−X2−Fe(3) angle for the singlet and triplet states. Contour drawings of the MOs for (1) a′ and a″ MOs of the 1A′ state for **A**(−2), (2) a′ and a″ MOs of the singlet 1A′ state for **A**(0), (3) a′ and a″ MOs of the 1A′ state for **B**(0), (4) a′ and a″ MOs of the triplet A′ state for **B**(2+). This material is available free of charge via the Internet at http://pubs.acs.org.

IC0499392